Z. Phys. C – Particles and Fields 48, 355–364 (1990)

Zeitschrift für Physik C Particles and Fields

A scalar-fermion model in the limit of infinitely heavy fermions

L. Lin, J.P. Ma, I. Montvay

Deutsches Elektronen-Synchrotron DESY, D-2000 Hamburg, Federal Republic of Germany

Received 20 June 1990

Abstract. As a first step in the non-perturbative study of a chiral $U(1)\otimes U(1)$ Yukawa-model with explicit mirror fermions the limit of infinite bare fermion mass is considered. Non-perturbative information is obtained from 14th order scalar hopping parameter expansion, which is confronted with high statistics numerical data. A remarkable universality of the upper bound for the renormalized quartic coupling is observed. A new kind of first order phase transition surface is localized, which is characterized by a large jump in the average field length.

1 Introduction

The existence of heavy fermions with masses of the order of at least a few hundred GeV is an interesting possibility in the Standard Model. The missing top quark can have a mass near 150–200 GeV, and a heavy fourth family with massive neutrino is still consistent with the experimental data [1, 2]. The mirror doubling of the fermion spectrum by three heavy mirror fermion families is not excluded either [3]. Even if the Yukawa-interaction is only medium strong at the electroweak energy scale, according to the perturbative renormalization group equations, it becomes stronger and stronger for higher energies. It can even become infinitely strong below the scale of quantum gravity, and this can be used as a basis for interesting theoretical models for the origin of the spontaneous electroweak symmetry breaking [4–6]. Therefore, the non-perturbative lattice investigation of strongly interacting Yukawa-models is highly actual and interesting.

An important aspect of non-perturbative lattice formulations of chiral Yukawa-models is that they have to deal with the consequences of the Nielsen–Ninomiya theorem [7], implying the mirror doubling of the fermion spectrum on the lattice. The mirror doubling, i.e. the existence of fermion pairs with the same quantum numbers but opposite chirality, is usually realized by "fermion doubler" states in different parts of the Brillouin-zone of momentum space. In the case of chiral Yukawa-models relevant in the electroweak sector the lattice formulation becomes more transparent if an explicit mirror doubling is introduced at the level of field components [8]. This doubling of the original chiral field content is convenient because of the existence of a phase with spontaneously broken mirror symmetry, where the mirror states are split in mass and are mixed with each other [8]. The interesting question is, whether the mirror fermion states can be decoupled, leaving a chirally asymmetric set of fermions in the physical spectrum [9, 10].

In the present paper we continue the study of chiral lattice Yukawa-models with explicit mirror fermions by doing the first step in the non-perturbative study of the simplest version, namely a model with chiral $U(1)\otimes U(1)$ symmetry. We investigate the limit of infinitely large off-diagonal bare fermion masses, which can be considered as the limit with "quenched" or "static" fermions. Different other lattice Yukawa-models have been investigated in the quenched approximation by several groups [11–13]. In these works the bare fermion mass was put equal to zero, whereas in our case the bare mass is infinite (the fermion hopping parameter is zero). At zero hopping parameter the static fermion determinant is not a constant (like e.g. in quenched QCD), but is a product of local factors depending on the bare Yukawa-couplings. If the product of bare Yukawa-couplings is infinite the value of the bare mass is not relevant, therefore in this case our model is similar to the limit of other effective scalar models at infinite bare Yukawa-coupling. (Such limits were considered, for instance, in [12, 14, 15]. For a recent review on non-perturbative Yukawa-models see [16].) The study of the effective scalar theory at infinitely heavy fermions is useful, because its phase structure can be expected to be continued in the interior of the parameter space of the full chiral $U(1)\otimes U(1)$-symmetric scalar-fermion model. The influence of the static fermion determinant on the cut-off dependent upper limit for the renormalized quartic coupling is also interesting (for references on upper limits see [17]).

The plan of this paper is as follows: after defining the model in Sect. 2, the 14th order scalar hopping parameter

expansion based on the results of Lüscher and Weisz [18] will be presented and compared to high statistics numerical Monte Carlo data in Sect. 3. The numerical investigation of the phase structure is included in Sect. 4. The last section contains a summary and some concluding remarks.

2 Lattice action

A prototype of the chiral Yukawa-model with explicit mirror fermions and $SU(2)\otimes SU(2)$ symmetry was considered in [8]. The corresponding $SU(2)\otimes U(1)$-symmetric model with mirror pairs of standard fermion families was defined in [19]. Here we consider the simplest version, namely a chiral $U(1)\otimes U(1)$-symmetric model with a mirror fermion pair (ψ_x, χ_x) and a complex scalar Higgs-field $\phi_x \equiv \phi_{R_x} + i\phi_{I_x}$. This model has many important qualitative features of the standard Higgs-Yukawa-sector since, for instance, from the point of view of anomalies only the $U(1)$ factor matters. The general lattice action of the $U(1)\otimes U(1)$ model can be written as

$$\begin{aligned} S = \sum_x \Big\{ & \mu_\phi \phi_x^+ \phi_x + \lambda(\phi_x^+ \phi_x)^2 - \kappa \sum_\mu \phi_{x+\hat{\mu}}^+ \phi_x \\ & + \mu_{\psi\chi}[(\bar{\chi}_x \psi_x) + (\bar{\psi}_x \chi_x)] - \sum_\mu [K_\psi(\bar{\psi}_{x+\hat{\mu}} \gamma_\mu \psi_x) \\ & + K_\chi(\bar{\chi}_{x+\hat{\mu}} \gamma_\mu \chi_x)] + K_r \sum_\mu [(\bar{\chi}_x \psi_x) - (\bar{\chi}_{x+\hat{\mu}} \psi_x) \\ & + (\bar{\psi}_x \chi_x) - (\bar{\psi}_{x+\hat{\mu}} \chi_x)] + G_\psi(\bar{\psi}_x [\phi_{R_x} - i\gamma_5 \phi_{I_x}] \psi_x) \\ & + G_\chi(\bar{\chi}_x [\phi_{R_x} + i\gamma_5 \phi_{I_x}] \chi_x) \Big\}. \end{aligned} \tag{1}$$

Here the normalization of the fields is left general, x is a lattice point and the sum $\sum_\mu$ runs over eight directions of the neighbours. A convenient normalization of the fields, which will be used in this paper, is defined by

$$\begin{aligned} & \mu_\phi = 1 - 2\lambda; \quad K_\psi = K_\chi \equiv K; \quad K_r \equiv rK; \\ & \bar{\mu} \equiv \mu_{\psi\chi} + 8rK = 1. \end{aligned} \tag{2}$$

In the present paper we consider the limit of zero fermion hopping parameter $K = 0$. In this case the fermionic part of the action $S_{\psi\chi\phi}$ can be written as

$$S_{\psi\chi\phi} = \sum_x \bar{\Psi}_x Q(\phi_x) \Psi_x \tag{3}$$

where the fermion field $\Psi_x \equiv (\psi_x, \chi_x)$ stands for the mirror pair, and the $8\otimes 8$ fermion matrix Q is given in a $2\otimes 2$ block notation by

$$Q(\phi_x) = \begin{pmatrix} G_\psi \phi_x^+ & 0 & 1 & 0 \\ 0 & G_\psi \phi_x & 0 & 1 \\ 1 & 0 & G_\chi \phi_x & 0 \\ 0 & 1 & 0 & G_\chi \phi_x^+ \end{pmatrix}. \tag{4}$$

This is on a chiral basis, that is $\gamma_5 = \mathrm{diag}(1, 1, -1, -1)$.

After integrating out the fermionic Grassmann variables the scalar path integral involves the fermion determinant

$$\prod_x \det Q(\phi_x) = \prod_x (G_\psi G_\chi \phi_x^+ \phi_x - 1)^4. \tag{5}$$

In a forthcoming publication [20] we shall numerically investigate the chiral $U(1)\otimes U(1)$ Yukawa-model (1) by using the hybrid Monte Carlo algorithm for dynamical fermions [21]. This method requires the duplication of the fermion spectrum by adding a second set of "flavours" having, instead of Q, the fermion matrix Q^+. This means that in the flavour-doubled model there are two mirror pairs of fermions. (In fact, due to the adjoint, the ψ-field of the second flavour is a "mirror-field" with respect to the ψ-field of the first flavour.) In the limit of zero fermion hopping parameter $K = 0$ the fermion determinant becomes

$$\prod_x \det [Q(\phi_x)^+ Q(\phi_x)] = \prod_x (G_\psi G_\chi \phi_x^+ \phi_x - 1)^8. \tag{6}$$

Since we want to apply the results of this work in [20], we shall consider also here the determinant in (6) instead of (5). Let us emphasize that this flavour doubling is of purely technical origin. The model defined by the action (1) is a perfectly honorable one. It can be investigated, for instance, by a non-perturbative fermion hopping parameter expansion. Even its fermion determinant is positive in the symmetric phase near $K = 0$. (In the broken phase the determinant of the original model is not positive definite but, of course, the flavour-doubled determinant $\det(Q^+ Q)$ is.)

The effective scalar action containing the logarithm of the fermion determinant (6) is

$$\begin{aligned} S_{\mathrm{eff}} = \sum_x \Big\{ & \phi_x^+ \phi_x + \lambda(\phi_x^+ \phi_x - 1)^2 \\ & + 8 \log |1 - G_\psi G_\chi \phi_x^+ \phi_x|^{-1} - \kappa \sum_\mu \phi_{x+\hat{\mu}}^+ \phi_x \Big\}. \end{aligned} \tag{7}$$

In the present paper we shall investigate the effective scalar model defined by this lattice action. It depends on the bare Yukawa-couplings only through the product $GG \equiv G_\psi G_\chi$. At vanishing GG it reduces to the $O(2)$-symmetric (or equivalently $U(1)$-symmetric) two-component ϕ^4 model (4-dimensional "xy-model"). At $GG = \infty$, after appropriately redefining the field normalizations, our model becomes similar to the infinite bare Yukawa-coupling limit of some other lattice Yukawa-models [12, 14, 15].

A qualitatively important property of the effective scalar action (7) is the appearance of the infinite logarithmic singularity at $GG|\phi_x|^2 = 1$. This corresponds to a very strong (high order) zero in the scalar path integral. This zero is, however, partly or completely compensated in the fermionic expectation values which involve the inverse of the fermion matrix (again in a $2\otimes 2$ block notation):

$$\begin{aligned} Q(\phi_x)^{-1} = & (G_\psi G_\chi \phi_x^+ \phi_x - 1)^{-1} \\ & \cdot \begin{pmatrix} G_\chi \phi_x & 0 & -1 & 0 \\ 0 & G_\chi \phi_x^+ & 0 & -1 \\ -1 & 0 & G_\psi \phi_x^+ & 0 \\ 0 & -1 & 0 & G_\psi \phi_x \end{pmatrix}. \end{aligned} \tag{8}$$

A complete compensation of the zero in the scalar path integral occurs at the maximum possible number of fermions in one point. In the flavour-doubled model this

means an expectation value $(\bar{\Psi}_x \Psi_x)$[16]. This phenomenon is quite analogous to the effect of fermion zero modes appearing in gauge theories in an instanton field [22]. In the present context the zero modes make the computation of (static) fermion expectation values more difficult, because of the essential difference in the path integral measure. For instance, a Monte Carlo updating with the effective scalar action in (7) does practically never probe the vicinity of the zero modes, hence the numerical calculation of fermionic expectation value would be very inefficient (especially for higher powers of the fermion fields). Therefore, in the present paper we shall only consider purely scalar expectation values.

3 Scalar hopping parameter expansion

A useful non-perturbative analytical tool is the expansion in powers of the scalar hopping parameter κ. This corresponds to the "high temperature expansion" in statistical physics models [23]. It has been used by Lüscher and Weisz in their approximate analytical solution of the $O(n)$-symmetric ϕ^4 models [24]. They worked out the combinatorial ingredients of the κ-expansion up to 14th order by using "linked cluster expansion" techniques [18]. These are available in form of a computer file and can be used to determine the expansion coefficients in an $O(n)$-symmetric scalar model with arbitrary one-site potential. The κ-expansion is expected to give a good approximation in the symmetric phase not very close to the critical line of the symmetry breaking phase transition, where the scalar boson mass in lattice units satisfies, say, $m_R \geqq 0.5$.

For the determination of the renormalized mass (m_R), renormalized coupling (g_R) and field renormalization constant (Z_R) one considers the susceptibilities χ_2, μ_2 and χ_4. Denoting the real field components by ϕ_{ax} $(a = R, I)$ and the number of lattice points by N, these are defined by connected expectation values $\langle \cdots \rangle_c$ as

$$\frac{1}{N} \sum_{x_1, x_2} \langle \phi_{a_1 x_2} \phi_{a_2 x_2} \rangle_c = \delta_{a_1 a_2} \chi_2$$

$$\frac{1}{N} \sum_{x_1, x_2} (x_1 - x_2)^2 \langle \phi_{a_1 x_1} \phi_{a_2 x_2} \rangle_c = \delta_{a_1 a_2} \mu_2$$

$$\frac{1}{N} \sum_{x_1, x_2, x_3, x_4} \langle \phi_{a_1 x_1} \phi_{a_2 x_2} \phi_{a_3 x_3} \phi_{a_4 x_4} \rangle_c = \tfrac{1}{3}(\delta_{a_1 a_2}\delta_{a_3 a_4} + \delta_{a_1 a_3}\delta_{a_2 a_4} + \delta_{a_1 a_4}\delta_{a_2 a_3}) \chi_4 . \tag{9}$$

The relations to the renormalized quantities are:

$$m_R^2 = 8 \frac{\chi_2}{\mu_2}; \quad Z_R = 8 \frac{(\chi_2)^2}{\mu_2}; \quad g_R = -64 \frac{\chi_4}{(\mu_2)^2}. \tag{10}$$

Let χ stand for χ_2, μ_2 or χ_4 and let us write the 14th order scalar hopping parameter expansion in infinite volume as

$$\chi = \sum_{L=0}^{14} \chi^{(L)} \frac{(2\kappa)^L}{L!}. \tag{11}$$

The coefficients $\chi^{(L)}$ are given by

$$\chi^{(L)} = \sum_i \mathring{m}_2^{N(i,1)} \mathring{m}_4^{N(i,2)} \cdots \mathring{m}_{18}^{N(i,9)} \cdot \{P(i,0) + P(i,1)2 + P(i,2)2^2 + \cdots + P(i,7)2^7\} \tag{12}$$

where

$$\mathring{m}_{2k} = \frac{1}{2^k k!} \cdot \frac{J_{1+2k}}{J_1} \tag{13}$$

and J_k is the following integral:

$$J_k = \int_0^\infty dx\, x^k e^{-u(x)}. \tag{14}$$

Here u denotes the single-site potential which, according to (7), is

$$u(x) = x^2 + \lambda(x^2 - 1)^2 + 8 \log |1 - G_\psi G_\chi x^2|^{-1}. \tag{15}$$

The numbers $N(i, j)$ and the coefficients $P(i, j)$ were worked out by Lüscher and Weisz [18]. The one-site integrals (14) can be evaluated numerically without problems. An example of the expansion coefficients at $\lambda = 1.0$ and $GG = 2.0$ is given in Table 1. An estimate of the critical scalar hopping parameter $\kappa_c(\lambda, GG)$ can be obtained, for instance, from the ratios $\chi_2^{(L-1)}/\chi_2^{(L)}$ of the expansion coefficients of the susceptibility χ_2. A better way is, however, to first transform the κ-series into power series in the variable v defined by

$$v = \frac{1}{2} \frac{\partial}{\partial \kappa} \ln \{ \int d\phi_1 d\phi_2 \exp [2\kappa \phi_1 \phi_2 - u(\phi_1) - u(\phi_2)] \} \tag{16}$$

L	$2^L \chi_2^{(L)}/L!$	$2^L \mu_2^{(L)}/L!$	$2^L \chi_4^{(L)}/L!$
0	1.28162273567749629	0.00000000000000000	-2.37275249482262840
1	26.2809093856875116	26.2809093856875116	-194.622306784011599
2	474.041273466298207	1077.83075145527084	-9187.51262650855460
3	8470.43765154776338	30572.3959919867339	-336972.314188083430
4	148679.294294903782	749336.363319444703	-10623518.0237211734
5	2604645.50916115567	16919075.3756249063	-303068726.394580126
6	45313279.2924877293	363025126.733940005	-8046225512.45104313
7	787595575.799141467	7516356382.12631607	-202412434142.887100
8	13639906221.8475151	151663696729.061890	-4881687015081.74805
9	236091476772.776138	3000024536927.46387	-113824209590282.914
10	4077671618171.17187	58428257061388.2617	-2581339178546899.75
11	70402717447091.7383	1123646109850887.25	-57200047446746501.0
12	1213809133591099.31	21386298745822485.0	-1242819376261315070
13	20922020708512059.0	403501797482870496.	-26551619137479991300
14	360266048400498016.	7556880972703807740	-558993250856086077000

Table 1. The expansion coefficients of χ_2, μ_2 and χ_4 at $\lambda = 1.0$, $GG = 2.0$

Table 2a–e. The results of the scalar hopping parameter expansion for $m_R = 0.5$ at **(a)** $\lambda = 0.01$, **(b)** $\lambda = 0.1$, **(c)** $\lambda = 1.0$, **(d)** $\lambda = 10.0$ and **(e)** $\lambda = 100.0$ as a function of GG. κ_c is the critical value, κ in the last column is the value where the renormalized mass $m_R = 0.5$

(a)

GG	κ_c	Z_R	g_R	κ
0.00	0.128396(5)	4.020(2)	3.37(5)	0.12437
0.10	0.24112(4)	2.1427(7)	5.8(1)	0.23333
0.20	0.235(8)	2.10(5)	-956	0.23312
0.30	0.0593(1)	7.7(2)	-692	0.058586
0.40	0.0180628(5)	28.76(4)	34(3)	0.017256
0.50	0.015821(1)	32.80(7)	39(3)	0.015047
0.60	0.016070(1)	32.29(7)	39(3)	0.015280
0.70	0.016401(1)	31.63(7)	39(3)	0.015595
0.80	0.016678(1)	31.11(7)	39(3)	0.015859
0.90	0.016902(1)	30.70(7)	39(3)	0.016074
1.00	0.017087(1)	30.37(7)	39(3)	0.016250
1.10	0.017241(1)	30.09(7)	39(3)	0.016397
1.20	0.017372(1)	29.87(7)	39(3)	0.016562
1.30	0.017484(1)	29.68(7)	39(3)	0.016629
1.40	0.017581(1)	29.51(7)	39(3)	0.016722
1.50	0.017666(1)	29.37(7)	39(3)	0.016803
1.60	0.017742(1)	29.25(7)	39(3)	0.016877
1.70	0.017808(1)	29.14(7)	39(3)	0.016939
1.80	0.017868(1)	29.04(7)	39(3)	0.016996
1.90	0.017922(1)	28.95(7)	39(3)	0.017047
2.00	0.017971(1)	28.87(7)	39(3)	0.017094

(b)

GG	κ_c	Z_R	g_R	κ
0.00	0.14633(2)	3.53830(1)	14.9(8)	0.14121
0.10	0.24369(4)	2.1231(4)	10.5(4)	0.23543
0.20	0.3619(2)	1.4304(2)	10.5(4)	0.34943
0.30	0.362(8)	1.39(1)	-477	0.35804
0.40	0.1337(3)	3.2(2)	-1818	0.13267
0.50	0.04189(1)	12.3661(6)	14(1)	0.040425
0.60	0.027096(1)	19.2(4)	38(3)	0.025801
0.70	0.025943(2)	20.0(5)	40(3)	0.024662
0.80	0.026200(2)	19.8(5)	40(3)	0.024901
0.90	0.026577(2)	19.5(5)	40(3)	0.025260
1.00	0.026920(2)	19.3(5)	40(3)	0.025586
1.10	0.027213(2)	19.1(5)	40(3)	0.025866
1.20	0.027464(2)	18.9(4)	40(3)	0.026105
1.30	0.027680(2)	18.7(4)	40(3)	0.026311
1.40	0.027868(2)	18.6(4)	40(3)	0.026490
1.50	0.028032(2)	18.5(4)	40(3)	0.026646
1.60	0.028177(2)	18.4(4)	40(3)	0.026785
1.70	0.028306(2)	18.3(4)	40(3)	0.026908
1.80	0.028422(2)	18.3(4)	40(3)	0.027019
1.90	0.028526(2)	18.2(4)	40(3)	0.027118
2.00	0.028620(2)	18.1(4)	40(3)	0.027208

(c)

GG	κ_c	Z_R	g_R	κ
0.00	0.17691(2)	2.935(3)	30(2)	0.16944
0.10	0.23285(3)	2.230(2)	26(2)	0.22348
0.20	0.31026(6)	1.6725(8)	23(1)	0.29824
0.30	0.4054(1)	1.2795(4)	21(1)	0.39011
0.40	0.5123(1)	1.0119(2)	19(1)	0.49342
0.50	0.6212(4)	0.83376(4)	13(2)	0.59920
0.60	0.557(5)	0.89(1)	-327	0.54899
0.70	0.3057(8)	1.48(1)	-1162	0.30308
0.80	0.1416(1)	3.5666(2)	-76	0.13848
0.90	0.07543(1)	6.887(7)	28(2)	0.072350
1.00	0.058912(2)	8.81(2)	37(3)	0.056107
1.10	0.055599(4)	9.33(2)	40(3)	0.052856
1.20	0.055254(5)	9.39(2)	40(3)	0.052504
1.30	0.055594(5)	9.33(2)	40(3)	0.052821
1.40	0.056075(5)	9.25(2)	40(3)	0.053276
1.50	0.056557(5)	9.18(2)	40(3)	0.053734
1.60	0.057004(5)	9.10(2)	40(3)	0.054160
1.70	0.057410(5)	9.03(2)	40(3)	0.054546
1.80	0.057777(5)	8.98(2)	40(3)	0.054895
1.90	0.058108(5)	8.93(2)	40(3)	0.055211
2.00	0.058408(5)	8.88(2)	40(3)	0.055497

(d)

GG	κ_c	Z_R	g_R	κ
0.00	0.15707(1)	3.303(8)	40(3)	0.14930
0.10	0.16455(1)	3.153(7)	40(3)	0.15643
0.20	0.17451(1)	2.973(7)	39(3)	0.16592
0.30	0.18786(1)	2.762(6)	39(3)	0.17864
0.40	0.20560(1)	2.524(7)	39(3)	0.19555
0.50	0.22867(2)	2.269(5)	39(3)	0.21755
0.60	0.25769(2)	2.014(4)	39(3)	0.25522
0.70	0.29296(2)	1.772(4)	38(3)	0.27888
0.80	0.33395(1)	1.554(3)	38(3)	0.31806
0.90	0.35291(3)	1.471(2)	32(2)	0.33768
1.00	0.21291(6)	2.4345(2)	16.7(7)	0.20521
1.10	0.115243(3)	4.506(9)	37(3)	0.10985
1.20	0.100402(8)	5.17(1)	40(3)	0.095401
1.30	0.099799(9)	5.20(1)	40(3)	0.094782
1.40	0.10093(1)	5.14(1)	40(3)	0.095853
1.50	0.10219(1)	5.08(1)	40(3)	0.097035
1.60	0.10331(1)	5.02(1)	40(3)	0.098110
1.70	0.10431(1)	4.97(1)	40(3)	0.099057
1.80	0.10518(1)	4.93(1)	40(3)	0.099891
1.90	0.10596(1)	4.89(1)	40(3)	0.10063
2.00	0.10665(1)	4.86(1)	40(3)	0.10128

(e)

GG	κ_c	Z_R	g_R	κ
0.00	0.15134(1)	3.426(9)	41(3)	0.14370
0.10	0.15202(1)	3.411(9)	41(3)	0.14434
0.20	0.15287(1)	3.392(9)	41(3)	0.14515
0.30	0.15397(2)	3.368(9)	41(3)	0.14619
0.40	0.15543(2)	3.336(8)	41(3)	0.14758
0.50	0.15743(2)	3.294(8)	41(3)	0.14948
0.60	0.16028(2)	3.235(8)	41(3)	0.15218
0.70	0.16445(2)	3.153(8)	41(3)	0.15614
0.80	0.17059(2)	3.040(8)	41(3)	0.16197
0.90	0.17922(2)	2.893(8)	41(3)	0.17016
1.00	0.15637(1)	3.317(8)	40(3)	0.14861
1.10	0.12974(1)	4.00(1)	41(3)	0.12318
1.20	0.13289(1)	3.90(1)	41(3)	0.12617
1.30	0.13515(1)	3.84(1)	41(3)	0.12831
1.40	0.13679(1)	3.79(1)	41(3)	0.12987
1.50	0.13802(1)	3.76(1)	41(3)	0.13104
1.60	0.13896(1)	3.732(9)	41(3)	0.13193
1.70	0.13971(1)	3.712(9)	41(3)	0.13264
1.80	0.14031(1)	3.696(9)	41(3)	0.13321
1.90	0.14080(1)	3.683(9)	41(3)	0.13368
2.00	0.14121(1)	3.672(9)	41(3)	0.13407

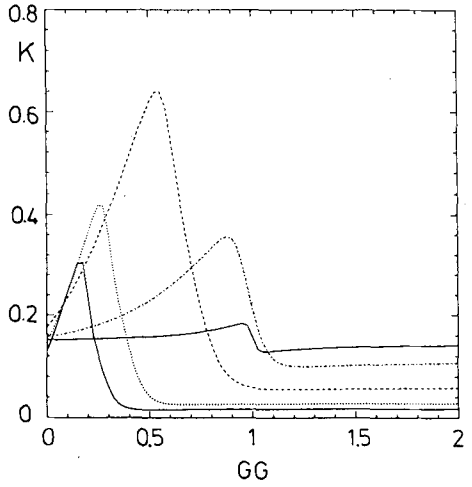

Fig. 1. The critical lines for fixed $\lambda = 0.01, 0.1, 1.0, 10.0$ and 100.0 as obtained from the 14th order scalar hopping parameter expansion. The dotted curve corresponds to $\lambda = 0.1$, the dashed one to $\lambda = 1.0$, the dashed-dotted to $\lambda = 10.0$, whereas $\lambda = 0.01$ and $\lambda = 100.0$ are represented by full curves. (The flatter one is $\lambda = 100.0$.)

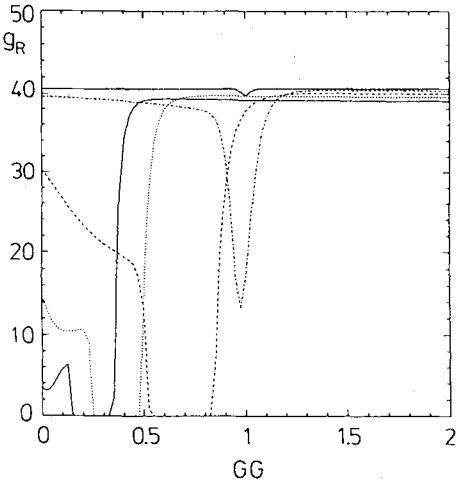

Fig. 2. The value of the renormalized coupling g_R for $m_R = 0.5$ in the symmetric phase at $\lambda = 0.01, 0.1, 1.0, 10.0$ and 100.0 as obtained from the 14th order scalar hopping parameter expansion. The dotted curve corresponds to $\lambda = 0.1$, the dashed one to $\lambda = 1.0$, the dashed-dotted to $\lambda = 10.0$, whereas $\lambda = 0.01$ and $\lambda = 100.0$ are represented by full curves. (The flatter one is $\lambda = 100.0$.)

and use the ratios of the expansion coefficients in v [24]. The asymptotic behaviour of these ratios is correlated with the form of the singularity of χ_2 at κ_c. The most precise values of $\kappa_c(\lambda, GG)$ can, therefore, be obtained if one assumes a specific form of the singularity corresponding to the scaling laws near the expected Gaussian fixed point. However, both the introduction of v and the assumption of the scaling law give only small corrections. Already the naive estimates based on the original ratios $\chi_2^{(L-1)}/\chi_2^{(L)}$ are quite good. The main effect of the corrections is that the estimated errors become smaller. The obtained critical lines for $\lambda = 0.01, 0.1, 1.0, 10.0$ and 100 are shown in Fig. 1. The errors on κ_c are in most cases so small that they are invisible on the scale of the plot. Exceptions are a few points in the region where, for fixed λ, κ_c decreases as a function GG. (For the numerical values of κ_c see Table 2a–e.)

The most important information one can obtain from the scalar hopping parameter expansion is the behaviour of the renormalized quantities near the edge of the scaling region. The experience in pure scalar ϕ^4 models shows that the 10–14th order expansion is quite accurate in the region where the renormalized mass is not smaller than $m_R \cong 0.25 - 0.5$. This is supported by high statistics numerical simulations [25] showing that in this region the scale breaking lattice artifacts are already small and the perturbative scaling behaviour starts to set in: the pure ϕ^4-model behaves as a quasi-continuum theory with finite cut-off.

In order to check this behaviour also in our effective scalar theory including the static fermion determinant, we calculated the value of the renormalized coupling on the surface where $m_R = 0.5$ (see Table 2a–e) and compared it in a few points to numerical simulation data with high statistics. The Monte Carlo simulations were performed by the Metropolis algorithm. In order to be able to determine the renormalized coupling with good accuracy, we have chosen the lattice size carefully. According to the experience of previous ϕ^4 calculations in the symmetric phase [25], the optimal lattice size for the given mass $m_R = 0.5$ is $8^3 \cdot 12$. This is because on larger lattices the statistical errors of g_R are too large. On small lattices, on the other hand, the finite size effects are too strong. Therefore, we have chosen an $8^3 \cdot 12$ lattice and performed $4 \cdot 10^6$ sweeps in two points at, respectively, $\lambda = 0.1$ and $\lambda = 1.0$, and $2 \cdot 10^6$ sweeps in a third point with $\lambda = 100.0$. The corrections for finite volume effects were done by assuming 1-loop perturbative formulae. These were checked to work well in pure ϕ^4 models on similar lattices and at similar renormalized couplings [25]. The obtained results for the mass m, susceptibility χ_2 and

$$\lambda_4 \equiv m^4 \frac{\chi_4}{(\chi_2)^2} \tag{17}$$

are given in Table 3, together with the infinite volume extrapolations for m_R, Z_R and g_R. The renormalized couplings agree very well with the corresponding results of the κ-expansion in Table 2a–e. The modified wave function renormalization factors $Z'_R \equiv 2\kappa Z_R$ are, within a few percent, equal to 1 in the same way as in pure ϕ^4 models. In general, the effective scalar model behaves almost always quite similarly to pure ϕ^4 models if one goes near to the critical line. The exception is the

λ	GG	κ	m	χ_2	$-\lambda_4$	m_R	Z_R	g_R
0.10	1.0	0.0255	0.502(2)	75.1(3)	35(3)	0.503(2)	19.0(4)	40(4)
1.00	1.4	0.0530	0.511(2)	34.9(2)	35(3)	0.513(2)	9.2(2)	39(4)
100.	2.0	0.1340	0.509(8)	14.5(3)	50(19)	0.510(8)	3.8(4)	59(25)

Table 3. The results of the numerical simulation together with the infinite volume quantities extrapolated by the 1-loop perturbative formulae. The numbers in parentheses are error estimates in the last numerals

intermediate piece of the critical line near $GG = 0.5 - 1.0$ where, for fixed λ, the critical hopping parameter κ_c decreases as a function of GG. In this region, as it is shown by Table 2a–e and Fig. 2, the calculated couplings are negative. It will be discussed in detail in the next section that here the phase transition to the broken phase is of first order and, therefore, no continuum limit can be defined.

4 Phase structure

In this section, we present what we know about the phase structure of this $U(1)$ chiral Yukawa model at $K = 0$, i.e.: the infinitely heavy fermion limit. In this limit, the fermion determinant can be easily calculated analytically, and the effective action is given in (7).

There are two limiting cases which are worthy of immediate attention. When $GG = 0$, we get back the pure scalar $O(2)$ model, which has a critical line in the (κ, λ) plane, separating the symmetric phase and the broken symmetry phase. At $GG = \infty$, the action becomes the pure scalar $O(2)$ one minus a $\sum_x \log(\phi_x^+ \phi_x)^8$ term. If at the same time $\lambda = \infty$, the system goes back to the pure $O(2)$ model with fixed field length and has a critical point. So at least for $GG = \infty$ at large λ, we believe that the system should have a critical point at some κ-value.

The above observation leads us to believe that when GG is either small or large, the system should behave like an effective scalar field theory and have a second order phase transition line (in the (κ, GG) plane for fixed λ) along which the continuum limit can be taken.

Also, when $\lambda = \infty$, the field length is restricted to be one, hence the log term in the effective action becomes an irrelevant constant for any value of GG. We conclude that in this case the system undergoes a second order phase transition at a fixed κ for any value of GG.

When $\kappa = 0$, there is no coupling between fields on different lattice sites, therefore the partition function is analytic in GG and λ even when the volume is infinite. This means that there cannot be any phase transition along the $\kappa = 0$ axis and the system is always in the symmetric phase.

We carried out Monte Carlo simulations in exploring the phase structure on 8^4 lattice which is enough for qualitative understanding. Most of the runs were done at $\lambda = 1.0$. What was found about the phase structure in the regions mentioned above basically agrees with the expectations. Values of the critical κ at small and large GG also agree with those obtained from the scalar hopping parameter expansion (up to some small deviations presumably due to finite size effects).

However, at $\lambda = 1.0$, we also found very strong evidence for a first order transition at $GG = 0.3, 0.4, 0.5, 0.7, 0.8, 0.82$ and 0.83. The phase structure seems to be more complicated than expected (Fig. 3). At the first order phase transition we have obtained either strong hysteresis loops or two-peak structure in the histogram of the link variable l, where l is given by

$$l = \frac{1}{8V} \sum_{x,\mu} \phi_{x+\hat{\mu}}^+ \phi_x, \tag{18}$$

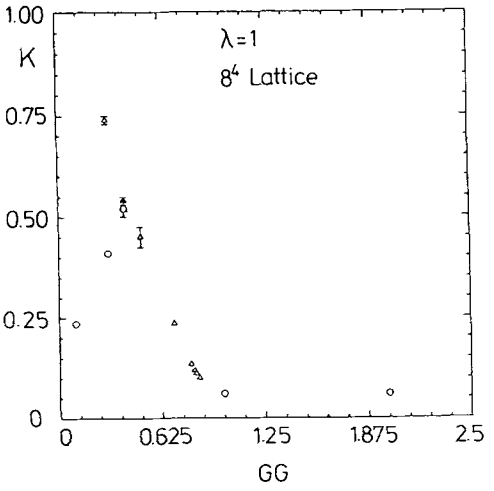

Fig. 3. The critical points at $\lambda = 1.0$ as obtained from Monte Carlo simulations on 8^4 lattice. Triangles represent first order phase transitions. Points without error bars have errors smaller than or comparable to the size of the symbol.

and $V \equiv N \equiv L^3 T$ is the number of lattice points.

We also measured the slope of the constrained effective potential at some intermediate points to make sure that the meta-stability or the two-peak histogram we saw is genuine (Table 4). The constrained effective potential on a finite lattice is defined as

$$\exp\{-V U_V(\bar{\phi})\} \equiv \int D[\phi_x] \delta\left(\bar{\phi} - \frac{1}{V}\sum_x \phi_x\right) e^{-S_{\text{eff}}} \tag{19}$$

where the effective action S_{eff} is given by (7). The derivative of the effective potential along the real direction in the $O(2)$ space can be worked out as

$$\frac{\partial U_V}{\partial \bar{\phi}_R} = (2 - 16\kappa)\bar{\phi}_R + \left\langle \frac{4\lambda}{V} \sum_x (\phi_x^+ \phi_x - 1)\phi_{Rx} \right\rangle_{\bar{\phi}} + \left\langle \frac{16 G_\psi G_\chi}{V} \sum_x \frac{\phi_{Rx}}{[1 - G_\psi G_\chi (\phi_x^+ \phi_x)]} \right\rangle_{\bar{\phi}} \tag{20}$$

where ϕ_R means the real component of the complex ϕ field, and $\langle\ \rangle_{\bar{\phi}}$ is the statistical average subject to the constraint represented by the δ-function in (19). Due to the underlying $O(2)$ symmetry, no generality is lost

Table 4. Data of the slope of the constrained effective potential measured on 8^4 lattice. U'_V means $\partial U_V / \partial \bar{\phi}_R$

λ	GG	κ	$\bar{\phi}_R$	$\bar{\phi}_I$	U'_V
1.0	0.3	0.74	0.8	0.0	-0.869(2)
1.0	0.3	0.74	1.2	0.0	2.630(1)
1.0	0.3	0.74	2.1	0.0	-2.014(3)
1.0	0.3	0.74	2.4	0.0	7.298(2)
1.0	0.8	0.135	0.1	0.0	1.301(1)
1.0	0.8	0.135	1.2	0.0	-0.247(8)
1.0	0.8	0.135	1.6	0.0	0.041(3)
1.0	0.83	0.1117	0.2	0.0	2.882(1)
1.0	0.83	0.1117	0.5	0.0	9.130(1)
1.0	0.83	0.1117	1.1	0.0	-0.207(3)
1.0	0.83	0.1117	1.4	0.0	-0.202(1)
1.0	0.83	0.1117	1.7	0.0	2.258(4)

when we choose the derivative with respect to the real component of the ϕ field. In Monte Carlo simulations, one just has to generate the probability distribution

$$P\{\phi\} \propto \delta\left[\bar{\phi} - \frac{1}{V}\sum_x \phi_x\right] e^{-S_{\text{eff}}} \tag{21}$$

which can be achieved by using the technique of the Lagrange multiplier in the hybrid Monte Carlo method [26]. We always set $\bar{\phi}_I = 0$ in our simulations.

We believe that we understand how this first order phase transition arises and will explain in the following.

When $\kappa = 0$, the effective action is a simple sum over the on-site action because there is no coupling between fields at different lattice sites. (Remember we are at $K = 0$.) Due to the presence of the log term which comes from the fermion determinant, the on-site action, when plotted against $\phi_x^+ \phi_x$, has a double-well structure with a singularity at $\phi_x^+ \phi_x = 1/GG$ between the two minima. As we turn on κ, that κ-term in (7) will align the spins at both minima. The energy density of the minima will decrease as the spins are more aligned. When the energy factor beats the entropy factor, the broken symmetry phase will have the lower free energy density and becomes the state of the system in the infinite volume limit. So the system goes from the symmetric phase to the broken symmetry phase through a seccond order phase transition. However, the one-site potential has a double-well structure and the energies of the two minima will depend on the value of GG. Therefore, there is also a possibility that the system jumps from one minimum to the other through a first order phase transition. After the κ-term is turned on, depending on the values of GG and κ, either the symmetric phase or the broken phase with spins from either minimum will have the lowest free energy density and defines the state of the system in the thermodynamic limit. Different mechanisms can come in to change the state of the system at different stages. So sometimes we have a second order phase transition and sometimes a first order one. This is basically what is behind the phase structure of the system.

We explore the phase structure by observing the system in the (κ, GG) plane at a fixed λ. The (κ, GG) plane can be divided into three regions according to the value of GG. In these regions the mechanism triggering the phase transition is qualitatively different. The three regions will later be called regions (A), (B) and (C) corresponding to small, large and intermediate values of GG, respectively. To make the presentation simpler, let us call the symmetric phase with shorter spins "symmetric phase (I)". The broken phase with shorter spins is called "broken phase (II)". The symmetric and broken phases with longer spins are called "symmetric phase (III)" and "broken phase (IV)", respectively. We use κ_t and κ_c to denote the values of κ at which first and second order phase transitions happen.

(1) Region (A)

In this region, GG is so small that the minimum with the smaller $\phi_x^+ \phi_x$ value is the global minimum at $\kappa = 0$. As κ increases from zero at a fixed GG, the spins with longer field length are more easily aligned. But the minimum with larger field length has a much higher energy density, therefore for smaller κ values the system will be in phase (I). Then the second order phase transition from phase (I) to phase (II) happens at some κ_c value. At some even larger κ_t value, the minimum with longer fields has lower free energy density. The system will jump from the previous minimum to this minimum, and undergoes a first order phase transition from phase (II) to phase (IV). After this, the system will continue to be in phase (IV), because it has longer fields and is energetically favoured by the κ term in the action.

When GG gets smaller, the difference between the two minima at $\kappa = 0$ is larger, which implies that κ_t grows as GG decreases. Also the first order transition should be stronger at smaller GG. The average field length of the other minimum becomes larger as GG decreases, therefore κ_c is smaller for smaller GG. In our Monte Carlo simulations at $\lambda = 1.0$ we have seen these qualitative behaviours. We think that the first order phase transition line can go all the way to the corner at $\kappa = \infty$ and $GG = 0$, because no matter how small GG is, we can eventually make phase (IV) be the phase with the lowest free energy density by increasing κ indefinitely. However, for some very small value of GG, the value of κ_t can be very large. Also, as far as the continuum limit is concerned, the first order phase transition line is not relevant, therefore we did not pursue the details of it.

(2) Region (B)

In this region, GG is large enough such that the minimum with the larger $\phi_x^+ \phi_x$ value becomes the global minimum at $\kappa = 0$. So, for small κ values, the system is in the symmetric phase (III). As the κ-term is turned on to align the spins, the system will go from phase (III) to phase (IV) through a second order phase transition. As κ gets even larger, phase (IV) will keep having the lowest free energy density, and the other minimum never has a chance to become the global minimum. Therefore in this region, we have only the second order phase transition line.

As GG grows to infinity, the field length at the global minimum will decrease gradually. This shows that κ_c should increase gradually as GG approaches infinity. We also see this qualitative behaviour in our simulations at $\lambda = 1.0$.

(3) Region (C)

In the region where the value of GG is intermediate, the minimum with shorter field length is still dominant at $\kappa = 0$. So, at small enough κ the system is in phase (I). However, the difference between the two minima becomes so small that when κ grows the higher minimum comes down before the spin-alignment at the lower minimum has occured. This implies that in this region, the first order phase transition from phase (I) to phase (IV) will happen first. The first order transition line in this region is the continuation of the first order line in region (A). As κ becomes even larger, the energy of the minimum

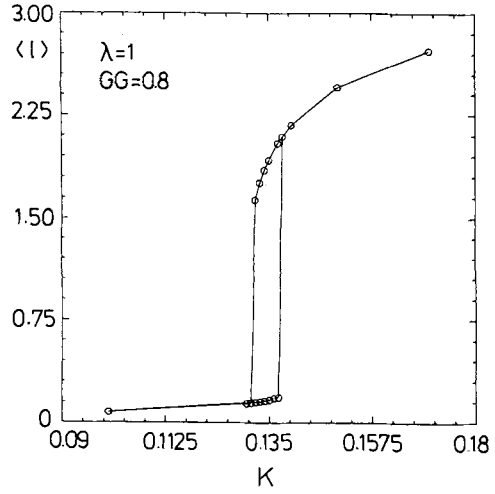

Fig. 4. Hysteresis loop of the link variable at $\lambda = 1.0$, $GG = 0.8$ on 8^4 lattice. Each point represents 20000 Metropolis sweeps with 5 hits per lattice site. Errors are smaller than or comparable to the size of the symbols

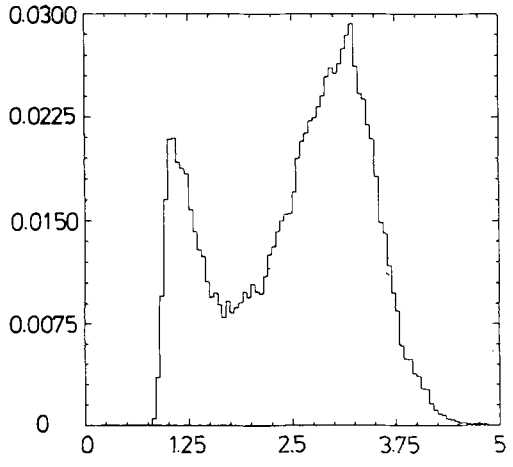

Fig. 5. The histogram of the link variable at $\lambda = 1.0$, $GG = 0.83$ and $\kappa = 0.1117$ on 8^4 lattice. The statistics is based on 80000 measurements. The normalizaion is chosen such that the total area under the curve is one

with the larger field length will drop faster, and phase (*IV*) will always have the lowest free energy density. Hence in the thermodynamic limit, we have only the first order phase transition.

When GG becomes larger in this region, the difference between the two minima at $\kappa = 0$ will be even smaller. So we expect that κ_t value will decrease as GG increases. Also, the first order phase transition should become weaker as GG increase. We see this qualitative behaviours in our simulations on the 8^4 lattice at $\lambda = 1.0$. There we obtained a weak hysteresis loop at $GG = 0.8$ (Fig. 4) and a double-peak structure in the histogram of the link variable l at $GG = 0.83$, $\kappa = 0.117$ on 8^4 lattice (Fig. 5). Compared to the hysteresis loop of l at $GG = 0.3$ (Fig. 6), we clearly see that the first order phase transition is becoming weaker and weaker as GG increases. At $GG = 0.85$, we did not see any two-peak structure in the histogram.

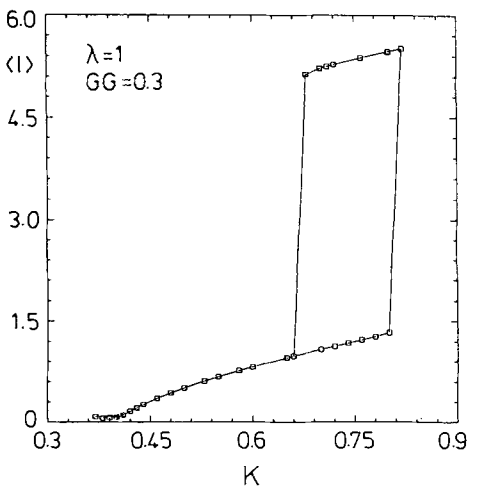

Fig. 6. A strong hysteresis loop of the link variable l at $\lambda = 1.0$, $GG = 0.3$ on 8^4 lattice. Each point has 30000 Metropolis sweeps with 5 hits per lattice site. Errors are smaller than or comparable to the size of the symbols

An important point is that we did not find any phase transition between the two symmetric phases with short and long spins. This implies that for small enough κ, as we go from region (*A*) to (*C*) and then to region (*B*) by increasing GG, the system will change from symmetric phase (*I*) to (*III*) in a gradual fashion. Hence, the second order phase transition line in region (*B*) is actually a continuation of the first order transition line in region (*C*). Somewhere along that line, the phase transition changes from first order to second order. We cannot be sure about exactly at which GG value this happens. However, based on our qualitative picture, we know that when we are well within region (*B*), (for $\lambda = 1.0$, this means a GG value substantially larger than one), the phase transition should be safely a second order one. There the mechanism for the phase transition is the spin alignment caused by the κ-term in the action. This is completely different from the mechanism triggering the phase transition in region (*C*). In order to verify this numerically, we did finite size scaling analysis on the specific heat C_V at $GG = 2.0$ and $\lambda = 1.0$, where C_V is defined as

$$C_V = V[\langle l^2 \rangle - \langle l \rangle^2]. \tag{22}$$

We first got some idea about the location of the phase transition point on $6^4, 8^4$ and 10^4 lattices and then measured C_V around the transition point on these lattices (Fig. 7). If the phase transition is of first order, then we expect that

$$C_V(L)_{\max} \propto L^{\alpha} \tag{23}$$

with $\alpha = 4.0$ in four dimension, where L is the linear size of the L^4 lattice, and the subscript max means the peak value of $C_V(L)$ vs. κ. If the system behaves like a pure scalar $O(n)$ model ($n = 2$ in our case), then the phase transition is of second order with $\alpha = 0$ (plus some logarithmic correction since we are in four dimensions). We obtained $\alpha = 0.20 \pm 0.10$ by fitting the data of the specific heat. (If we use data from 8^4 and 10^4 lattices only, we get $\alpha = 0.16 \pm 0.21$.) This clearly shows that the phase

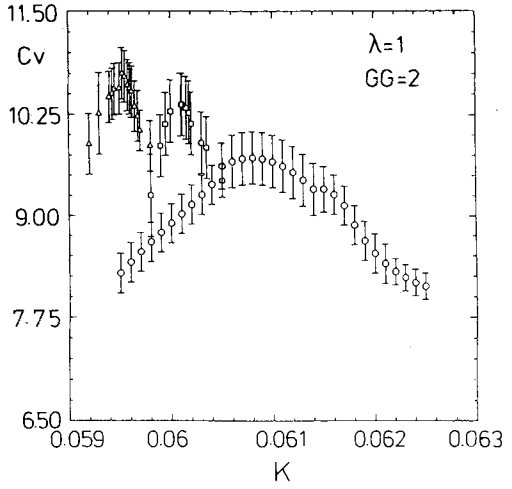

Fig. 7. Data of the specific heat measured in Monte Carlo simulations. Circles are on 6^4 lattice, while squares and triangles represent data on 8^4 and 10^4 lattices, respectively

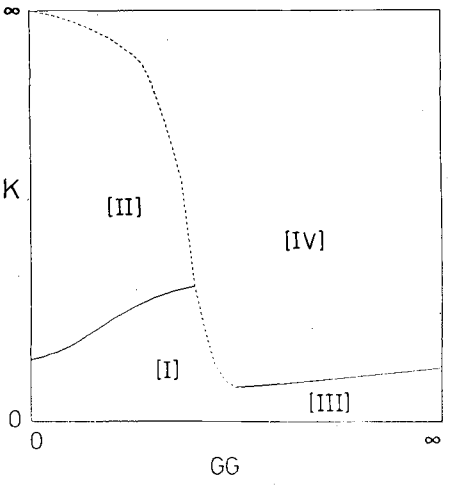

Fig. 9. A schematic plot of the phase diagram at strong λ (e.g.: $\lambda = 10.0$). The first order phase transition here is weaker than that in Fig. 8.

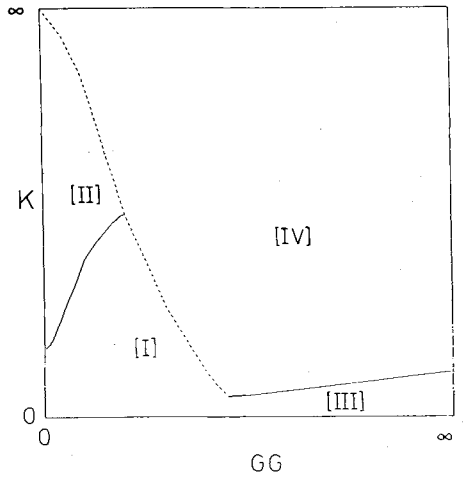

Fig. 8. A schematic plot of the phase diagram at weak λ (e.g.: $\lambda = 1.0$). Solid curves are the second order phase transition lines. The dash line depicts the first order phase transition. Regions corresponding to different phases are marked in the figure

transition is not a first order one, and is consistent with a Gaussian critical point instead. We believe that for GG greater than 2.0 at $\lambda = 1.0$, the phase transition is second order and the continuum limit can be taken around it.

The remaining question is how this phase structure at $\lambda = 1.0$ changes as we vary λ. If we go back to the one-site action at $\kappa = 0$, we will see how the distance (in field length) and the difference in energy density between the minima change as λ is changing qualitatively. From that, we expect that the first order phase transition appearing in both regions (A) and (C) becomes weaker as λ grows and finally disappears at $\lambda = \infty$. The "border" between regions (A) and (C) will shift to a larger GG value as λ grows and stops at $GG = 1.0$ when $\lambda = \infty$. The same happens to the "border" separating regions (B) and (C). The width of region (C) measured in GG becomes narrower and eventualy vanishes at $\lambda = \infty$. So, phase (II) and phase (IV) become the same in the $\lambda = \infty$ limit. This means that these two broken phases are analytically connected to each other. By looking how the field length of either minimum changes as λ varies, we can also qualitatively see that the second order phase transition lines in regions (A), (B) should become flatter and eventually join each other at $\lambda = \infty$ in such a way that the whole second order phase transition line becomes completely parallel to the $\kappa = 0$ axis in the (κ, GG) plane. Hence at $\lambda = \infty$, we do not have the first order phase transition, and κ_c for the second order phase transition is independent of GG. These features are schematically shown by Figs. 8 and 9. The qualitative statements about the second order phase transition line and the positions of borders between different regions have been verified by the κ-expansion. We have done simulations at $\lambda = 0.1, 2.0, 5.0, 6.0, 6.5, 7.0$ and 10.0 in region (C) on 8^4 lattice. Compared to the result at $\lambda = 1.0$, we do see that the first order transition is getting weaker and weaker as λ increases. At $\lambda = 6.5$, we are still able to obtain a weak hysteresis loop of l (at $GG = 0.9$). However, at $\lambda = 7.0$, no hysteresis loop or two-peak histogram can be found on 8^4 lattice. We believe that the phase transition in regions (A) and (C) should remain first order for all λ's (except for $\lambda = \infty$), because the mechanism triggering the phase transition from phase (I) to phase (IV) is the jump between two minima, which is quite different from spin alignment by the κ-term in the action. However, it is not easy to verify this numerically.

Based on this qualitative understanding of the phase structure, one can conclude that continuum limits can be taken at the critical κ_c both at small and large values of GG, i.e. in regions (A) and (B).

Note that the model has the symmetry $\kappa \to -\kappa$, $\phi_x \to (-1)^x \phi_x$. Therefore, in the negative κ-half-plane there is a phase transition between the symmetric phase and the anti-ferromagnetic phase.

In the future, as we move to nonzero K values, it will be very interesting to see how the first order phase transition hyper-surface goes as K varies. We think that in the small K region a K-expansion may give some information on that.

5 Discussion and summary

In the effective scalar model including the static fermion determinant of the $U(1)$ chiral Yukawa model the phase transition surface between the symmetric and broken phases has three different parts. At small and large values of the product of the Yukawa-couplings GG the numerical simulation data suggest second order phase transition, which is due to the alignment of the field by the nearest neighbour coupling. This is supported by the information obtained from the 14th order scalar hopping parameter expansion. In the intermediate region the transition becomes first order, as shown by strong hysteresis loops and double-peaked histograms. This first order transition is continued inside the broken phase. It is characterized by a jump of the system from a state with typically short fields to another state with longer fields. The broken phases with short and long fields are analytically connected to each other in the $\lambda = \infty$ plane, where the field length is frozen to 1, and the first order phase transition disappears (in the limit $\lambda \to \infty$ it shrinks to the point $GG = 1$, $\kappa = \kappa_c(\lambda = \infty)$). An interesting question is, how this first order phase transition is penetrating inside the parameter space with $K \neq 0$, in particular whether it also appears in the subspace describing the chiral $U(1)$ Yukawa-model in the broken symmetry phase with decoupled mirror fermions. We intend to investigate this in the future.

The point ($\lambda = \infty$, $GG = 1$, $\kappa = \kappa_c(\lambda = \infty)$) in the parameter space is rather interesting since, for instance, it is the endpoint of the lines separating the first order phase transition from the second order ones. Therefore, it could be an interesting non-trivial tricritical point. The investigation of its vicinity in the full Yukawa-model is one of the interesting questions for the non-perturbative study of this model with dynamical fermions [20].

Continuum limits can be defined near the second order parts of the phase transition surface. All non-perturbative information we obtained is consistent with the statement, that the model in the scaling region belongs to the equivalence class of two-component ϕ^4-models with $O(2)$ symmetry (and trivial continuum limit). In particular, the values of the renormalized coupling at the edge of the scaling region, obtained from the scalar hopping parameter expansion and checked by numerical simulations, are such that in the scaling region the interaction gets never really strong. The upper limit on the renormalized coupling at $m_R = 0.5$ is practically the same in this extended model as in the pure ϕ^4-model (roughly $g_R \leqq 40$). A remarkable feature is that this upper limit is reached not only at $\lambda = \infty$, but also at any other λ if the product of Yukawa-couplings GG is large enough. The independence of the upper limit from the Yukawa-couplings is another example of the unexpected universality of the upper limit for the renormalized quartic coupling in lattice ϕ^4 models. We investigated this upper limit only in the symmetric phase but, by the Lüscher–Weisz connection [24] between the scaling regions in the symmetric and broken phases, the universality is extended also to the broken phase.

Acknowledgements. We thank Gernot Münster for helpful discussions and for performing the finite volume corrections on our numerical data in Table III. The helpful advice of Martin Lüscher on the use of the results in [18] is gratefully acknowledged. The Monte Carlo calculations for this paper have been performed on the CRAY Y-MAP of HLRZ, Jülich.

References

1. J. Ellis, G.L. Fogli: Phys. Lett. 232B (1989) 139; G.L. Fogli, E. Lisi: Phys. Lett. 228B (1989) 389
2. D. Haidt: DESY preprint 89-073 (1989); Proceedings of the Madrid Europhysics Conference on HEP, 1989
3. I. Montvay: Phys. Lett. 205B (1988) 315; F. Csikor, I. Montvay: Phys. Lett. 231B (1989) 503; Proceedings of the Madrid Europhysics Conference on HEP, 1989
4. Y. Nambu: Enrico Fermi Institute preprint, 89-08 (1989)
5. V.A. Miransky, M. Tanabashi, K. Yamawaki: Mod. Phys. Lett. A4 (1989) 1043; Phys. Lett. B221 (1989) 177
6. W. Bardeen, C. Hill, M. Lindner: Phys. Rev. D41 (1990) 1647
7. H.B. Nielsen, M. Ninomiya: Nucl. Phys. B185 (1981) 20; errata: Nucl. Phys. B195 (1982) 541
8. I. Montvay: Phys. Lett. 199B (1987) 89
9. A. Borrelli et al.: Phys. Lett. 221B (1989) 360
10. A. Borrelli et al.: Nucl. Phys. B333 (1990) 335
11. J. Shigemitsu: Ohio State University preprints DOE/ER/01545-389, DOE/ER/01545-397
12. A. Hasenfratz, T. Neuhaus: Phys. Lett. 220B (1989) 435; A. Hasenfratz: Nucl. Phys. B (Proc. Suppl.) 9 (1989) 92
13. W. Bock et al.: Phys. Lett. 231B (1989) 283; W. Bock et al.: Phys. Lett. 232B (1989) 486
14. I-Hsiu Lee, J. Shigemitsu, R.E. Shrock: Nucl. Phys. B330 (1990) 225; B334 (1990) 265
15. M.A. Stefanov, M.M. Tsypin: Phys. Lett. 236B (1990) 344, Lebedev Institute preprint 90-028 (1990)
16. J. Smit: Amsterdam preprint, ITFA-89-31 (1989), to appear in the Proceedings of the International Conference Lattice '89, Capri
17. J. Jersák: HLRZ Jülich preprint 89-45 (1989), to appear in the Proceedings of the 8th INFN Eloisatron Project Workshop, Eric 1989
18. M. Lüscher, P. Weisz: Nucl. Phys. B300 [FS22] (1988) 325
19. I. Montvay: Nucl. Phys. B (Proc. Suppl.) 4 (1988) 443
20. K. Farakos et al.: DESY preprint 90-035
21. S. Duane, A.D. Kennedy, B.J. Pendleton, D. Roweth: Phys. Lett. 195B (1987) 216
22. G. 't Hooft, Phys. Rev. D14 (1976) 3432; erratum: Phys. Rev. D18 (1978) 2199
23. M. Wortis, in: Phase transitions and critical phenomena, Vol. 3, C. Domb, M.S. Green (eds.) London: Academic Press 1974
24. M. Lüscher, P. Weisz: Nucl. Phys. B290 [FS20] (1987) 25; Nucl. Phys. B318 (1989) 705; Nucl. Phys. B295 [FS21] (1988) 65
25. I. Montvay, P. Weisz: Nucl. Phys. B290 [FS20] (1987) 327; I. Montvay, G. Münster, U. Wolff: Nucl. Phys. B305 [FS23] (1988) 143; C. Frick et al.: Nucl. Phys. B331 (1990) 515
26. Y. Shen, J. Kuti, L. Lin, P. Rossi: Nucl. Phys. B (Proc. Suppl.) 9 (1989) 99